Fracture 1977, Volume 2, ICF4, Waterloo, Canada, June 19 - 24, 1977

PLASTIC DEFORMATION IN THE NECK OF α-Fe SINGLE CRYSTALS LEADING TO FRACTURE

R. N. Gardner and H. G. F. Wilsdorf*

INTRODUCTION

The relationship between macroscopic fracture and the state of internal dislocation structures just prior to fracture initiation, crack propagation and ligament separation is of vital importance in obtaining a fundamental understanding of the causes, progress, and nature of fracture. Therefore, the purpose of our investigation of the evolution of dislocation structures is the elucidation of (i) the causes of fracture initiation (ii) the dynamics of crack propagation and (iii) the ultimate strength of ligaments and their final mode of separation.

The method of approach has been *in situ* straining in the high voltage electron microscope (HVEM) of various types of both single crystals, and polycrystalline foils [1-3]. We should emphasize, however, that it is necessary to correlate the macroscopic behaviour of crystals with the microscopic observations of *in situ* experiments in the HVEM. Thus, in this communication our findings concerning the macroscopic characterization of the mode of fracture of small crystal filaments as well as their deformation histories are summarized for α-iron.

We recognize the importance of the deformation history in determining the ultimate strength and the final fracture mode of crystals. Certainly, the fracture of single crystals depends on dislocation structure, as is exemplified by the differences in two modes of failure: Crystals failing due to simple shear on a primary glide plane require the activation of only one slip system and no significant rotation, whereas the rupture of a similar crystal necessitates a more complex disposition of dislocations.

Currently, with respect to workhardening theories there has been little consideration given to the complex nature and disposition of dislocations after extensive elongations. Descriptions of dislocation structure existing in α-iron strained to moderate extensions [4] indicate that there must necessarily be a high dislocation density at the point of fracture.

A detailed analysis of the results of this investigation is consistent with the complicated dislocation structures expected at fracture. These tend to support the concept of a pattern of discrete steps required for fracture initiation of clean, bulk solids.

EXPERIMENTAL PROCEDURE

For this study, single crystal iron whiskers were prepared by the hydrogen reduction of ferrous halides. Ranging between 10-500 microns in diameter and about a centimeter in length, the crystals were found to be of various

*Department of Materials Science, University of Virginia, Charlottesville, Va 22901, U.S.A.

shapes, geometries, and orientations [5]. They were characterized both before and after deformation by observation in the scanning electron microscope (SEM) and through the use of the X-ray precession method. The precession method provides information concerning orientation, indexing of crystal faces and most importantly it enables the determination of the deformation character and geometrical history of these small crystals [6]. In addition to their observation in the SEM, the crystals were also observed during deformation, under the light microscope.

Crystals were strained to fracture in an INSTRON tensile testing machine, as well as in a bench straining device, at elongation rates varying from 10^{-7} cm/sec to 8.3 x 10^{-2} cm/sec. In addition, large ribbons on the order of 4-10 microns thick and 50 microns wide were strained *in situ* in the HVEM. The results from experiments with these ribbons will be further documented in a subsequent communication.

Some samples used in this study, and from which pertinent data was obtained, had initially been mounted in slotted supporting grips prior to straining. Also, some samples which were epoxied to glass capillaries and then coated with 300 Å of gold were viewed in the SEM. Crystals were in all cases handled immediately below kinked portions to insure that no defects to the crystals were introduced as a result of handling and that strain rate and fracture data obtained was for virgin, dislocation-free whiskers.

RESULTS AND DISCUSSION

Predeformation precession photographs indicate a high degree of overall crystalline perfection of the iron whiskers prepared for this study. While more than 100 crystals were strained in this investigation, all of the data obtained on each crystal was uniformly consistent with the results for all other crystals. Because these results are self-consistent in this communication we will limit ourselves to a few general comments regarding all crystallographic orientations followed by a detailed description of the macroscopic investigation of <110> oriented crystals.

It was noted that the elastic behaviour of many of these crystals was masked by the activation of a number of slip systems in the "microstrain" or stage "0" region. An example of this is given in Figure 1. Here, "unexpected {110} slip" is observed prior to establishment of slip on the primary {110} slip plane. This was determined by slip trace analysis of adjacent surfaces of the depicted crystal. The appearance of glide traces on the surfaces was found to be elongation rate dependent. The strengths of the crystals varied systematically with orientation and were in the range of 0.6-9 x 10^{8} (Pa). This is greater than the strengths of normal bulk single crystals, yet they were also determined to fail at stresses similar to those reported by Brenner [7] for iron whiskers thicker than 10 μm.

Plastic deformation preceding fracture was a complex phenomenon, as evidenced by the many slip anomalies observed. Three stage hardening was uniformly exhibited by the majority of crystals studied, as was 100% reduction in area, i.e., chisel point fracture. The chisel point fracture appeared "crystallographic" in nature. That is, edges of certain orientations were consistently along identical directions, and reductions in area repeatedly demonstrated the same geometric behaviour. An example of such behaviour is the fracture of crystals oriented in the <111> direction. A <110> crystal having a hexagonal cross-section is shown in

Figure 2. Figure 3 diagrammatically depicts the orientation of its crystal faces and the crystallography of the reduction in area.

The engineering stress-strain curves of <110> oriented crystals, whose failure geometry appeared in Figure 2, are plotted in Figure 4. True stress-strain curves were not plotted from load-time curves obtained from the INSTRON tensile testing machine because the assumption of uniform yielding along the length of the sample was not valid for these whiskers. Localized yielding was observed in most cases. All tests discussed here were performed at room temperature and at a constant cross head speed of 8.33 x 10^{-5} centimeters/second.

We note in Figure 4, variations in the hardening rate of these crystals. This was observed as being related to the number of active slip systems. The crystal depicted in Figure 2 had a hardening curve identical to that of A shown in Figure 4. From the deformation geometry it can be determined that there has been no distinguishable atomic displacement in any direction other than perpendicular to the {110} crystal face. This indicates that the only possible active Burgers vector is normal to the appropriate {110} face. With the aid of a cubic (110) standard stereographic projection it can be determined that the only possible active slip systems were $(112)[11\bar{1}]$ and $(11\bar{2})[111]$. Further verification of this fact may be obtained through the use of the precession method. Figure 5 indicates this lattice rotation. Increased hardening rates of samples B, C, and D are due to the additional activation of either the $(12\bar{3})[111]$ and $(123)[11\bar{1}]$ systems simultaneously and/or with further contributions of the $(21\bar{3})[111]$ and $(213)[11\bar{1}]$ slip systems acting together to cause only a slight change in deformation geometry. This phenomenon is evidenced by an indented line along the tensile axis, described here in Figure 6. Consideration has been given to the possibility that the line on the {110} crystal face is along an invariant plane of deformation. This, however, would necessitate the activation of several asymmetric slip systems. Precession photographs indicate that these particular systems are not active in these crystals. It can be concluded that the workhardening rates appear to be directly dependent upon the number of active slip systems. Table 1 includes labelled curves and lists the active slip systems responsible for the observed hardening behaviour. Also listed (see Table 2) are the initial Schmid factors for each system. The data obtained in these experiments suggests that the initial activation of additional slip systems may possibly be due to misorientation of the crystal in the grips.

Further results of the precession method indicate a symmetric rotation of volume elements with some rotating clockwise and some counter-clockwise about a specific normal to the tensile axis as indicated in Figure 3. This rotation is seen as being the consequence of an effective reduction in stored energy of cells found during the deformation processes. It is presumed then that dislocations move so as to screen each other's stress fields forming cells. These cells then shrink in size by the principle of similitude [8,9]. Due to the passage of dislocations through cells, the volume elements contained by a cell is being sheared. The incorporation of these glide dislocations into cell walls will then lead to the rotations observed. Thus, it is clear that the results of the precession method are in agreement with those predicted from cellular workhardening theory [10,11]. The rate of formation of cells and the rate of shrinkage is certainly dependent upon the number of active slip systems. This is consistent with the differences observed in the hardening curves as well as this investigation's determination of the dependence of slip trace depth on elongation rate [12].

The extension of the above to the final mode of deformation and ultimately to fracture, provides the logical sequence necessary for ductile fracture initiation. We might consider cell rotation to be limited to the saturation of the grid of screw dislocations that are found between two cells whose interface is perpendicular to the rotational axis. However, the angles of rotation are greater than what we might expect to see from the simple seizure of a dislocation grid. We further note that the lattice rotation is usually found to be toward the tensile axis except in those cases where asymmetric slip systems are active. The degree of rotation of the cells is invariably that amount necessary to align the original primary slip system with the tensile axis. This rotation is completed at the point of separation and covers the entire necked area.

Glide packet formation results in diffraction maxima which are discrete points, and these discrete points indicate various degrees of rotation for each packet. However, in the necked region the diffraction maxima are smoothly and continuously streaked, resulting from a uniform rotation of volume elements throughout the length of the necked region.

The effect of the grips on single crystal deformation has been considered and it is believed that only the lattice rotational grip effect will be of any significance in b.c.c. metals [5]. The significant effect is specifically the enhancement of the activation of the primary slip system as is confirmed by tests showing extended geometric softening of these crystals.

CONCLUSIONS

Certain relevant conclusions concerning the predeformation history may be inferred from the observations made and the data collected in this investigation. We note that the reduction in area at the fractured end on the crystals studied has not been the result of simple shear, but was produced by predictable sets of glide dislocations in accordance with the conditions imposed by the external geometries. Crystals of similar size and shape, but with their stress axes parallel to <110>, <111> and <211> respectively, exhibited a correspondingly systematical glide behaviour. The fracture of these crystals may be considered analagous to the failure of ligaments within a three-dimensional void sheet formed during the final phase of the fracture of a bulk crystal. Assuming a similarity in triaxial stresses between those in the unslipped region of our crystals and those in ligaments in bulk crystals, we may predict the glide geometry and dislocation structures which will result during the failure of the ligaments. We also recognize that the accommodation of large strains as well as the reduction in area is determined by the movement of dislocations on the order of a distance equal to that of the dislocation cell size.

Finally, we observe an apparent relationship between the extent of cell rotation in Stage III hardening and the initiation of fracture. The extent of the uniformity of cell development and similitude is then of fundamental importance in the understanding of the causes and nature of fracture.

ACKNOWLEDGEMENTS

The authors thank Professor D. Kuhlmann-Wilsdorf for her helpful criticisms and enlightening discussions. We thank the Metallurgy Branch of the Office of Naval Research, Arlington, Virginia for their support.

REFERENCES

1. BAUER, R. W., GEISS, R. H., LYLES, R. L. and WILSDORF, H. G. F., Fifth International Materials Science Symposium, University of California, Berkeley (Thomas, Ed.) p.85 (University of California Press, Berkely, California) 1972.
2. LYLES, R. L., Jr., and WILSDORF, H. G. F., Acta Met. 23, 1975, 269.
3. BAUER, R. W., LYLES, R. L., Jr., and WILSDORF, H. G. F., Zs. Metallkd. 63, 1972, 525.
4. NAGAKAWA, Johsei, SATO, A. and MESHII, M., Phil. Mag. 32, 1975, 1107.
5. GARDNER, R. N., M.S. Thesis, University of Virginia, 1975.
6. GARDNER, R. N. and HANSCOM, R. H., Mater. Sci. Eng., 22, 1976, 167.
7. BRENNER, S. S., J. Appl. Phys. 27, 1956, 1484.
8. KUHLMANN-WILSDORF, D., Trans. Met. Soc. AIME 224, 1962, 1047.
9. KUHLMANN-WILSDORF, D., "Workhardening" (Eds. J. P. Hirth and J. Wertman), Gordon and Breach, NY, 1968, 97.
10. KUHLMANN-WILSDORF, D., Met. Trans., 1, 1970, 3173.
11. KUHLMANN-WILSDORF, D., "Recent Progress in Understanding of Pure Metal and Alloy Hardening" in "Advances in Understanding of Monatomic and Cyclic Workhardening" (Eds. A. W. Thompson and R. Pelloix), AIME 1976, in press.
12. GARDNER, R. N. and WILSDORF, H. G. F., to be published.

Table 1

Tensile Axis	Crystal	Active Slip System
[110]	A	$(11\bar{2})[111], (112)[11\bar{1}]$
[110]	B	$(12\bar{3})[111], (123)[11\bar{1}], (11\bar{2})[111], (112)[11\bar{1}]$
[110]	C;D	$\{(12\bar{3})[111], (123)[11\bar{1}], (11\bar{2})[111]$ $(112)[11\bar{1}], (21\bar{3})[111], (213)[11\bar{1}]\}$

Table 2

For a tensile direction of [110]	
Slip System	Initial Schmid Factor
$(11\bar{2})[111]$	0.47
$(112)[11\bar{1}]$	0.47
$(12\bar{3})[111]$	0.46
$(21\bar{3})[111]$	0.46
$(213)[11\bar{1}]$	0.46
$(123)[11\bar{1}]$	0.46

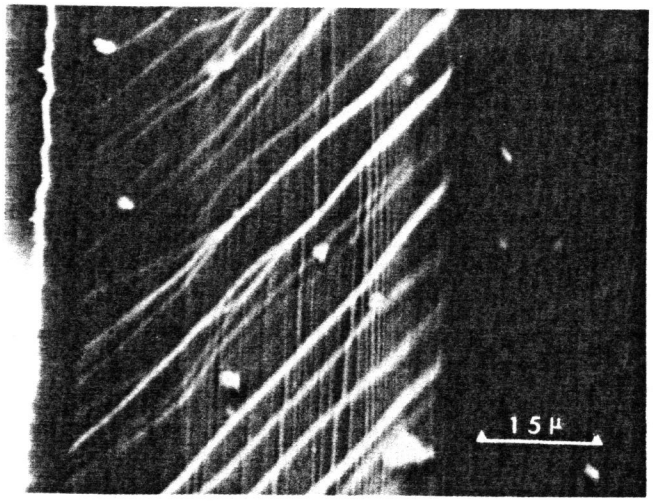

Figure 1 Slip Traces on the Surface of a <100> Tensile Sample. Note Coarse Lines have Displaced the Fine Initial Slip Lines

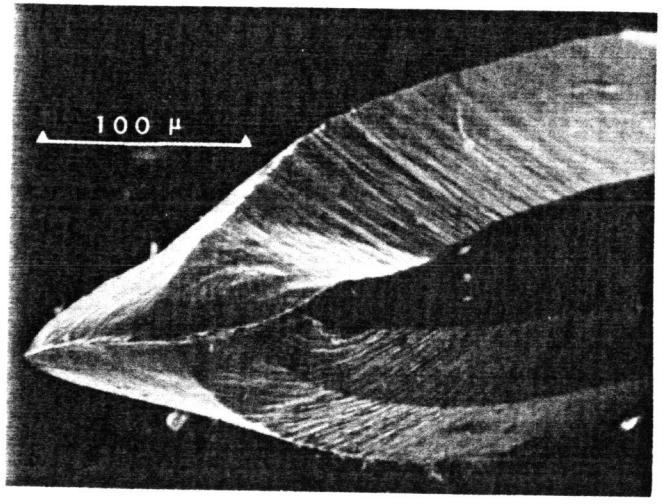

Figure 2 SEM Micrograph of the Fractured Tip of an α-Iron Whisker (<110>)

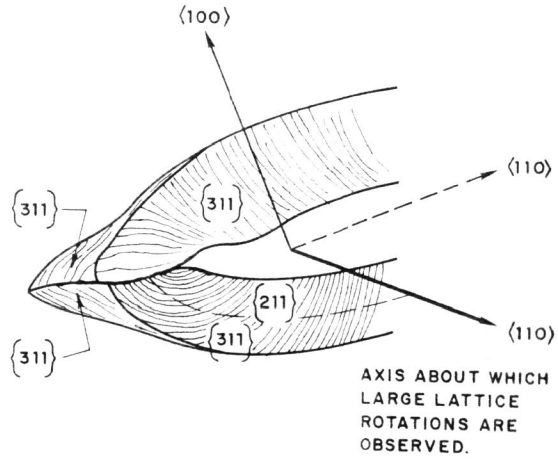

Figure 3 Diagram of a <110> Oriented Whisker Depicting the Crystallography of the Reduction in Area

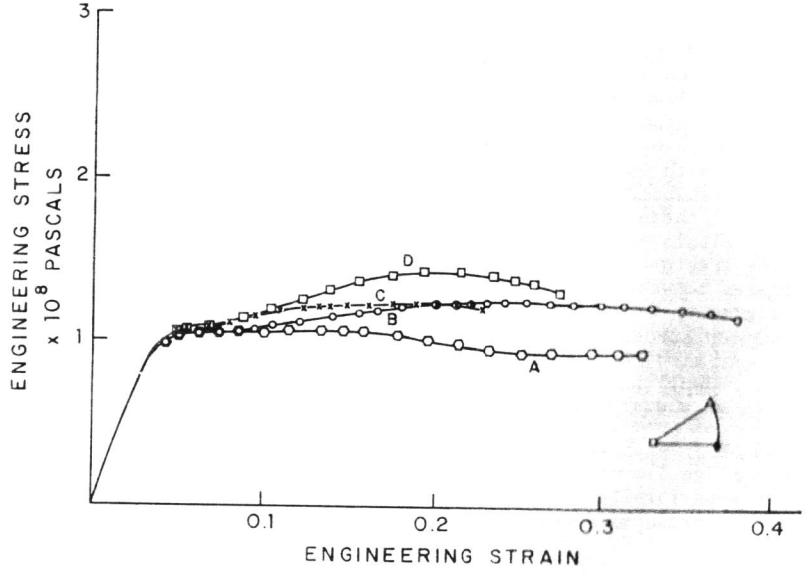

Figure 4 Engineering Stress-Strain Curves of Four <110> Oriented Crystals

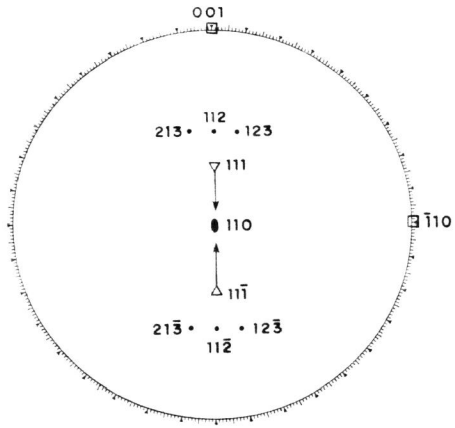

Figure 5 Stereographic Net Showing Observed Lattice Rotations

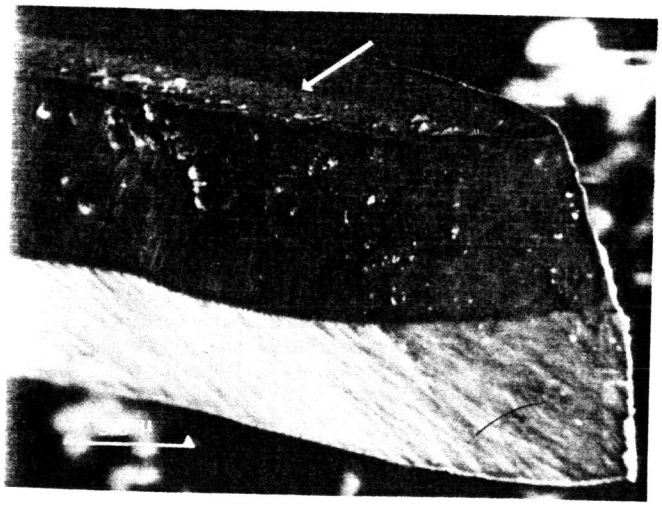

Figure 6 The Line on the Smooth Face is Indicative of the Activation of Another Burgers Vector Belonging to a Slip System Other than {211} <111>